J. Fluid Mech. (1967), *vol.* 29, *part* 4, *pp.* 705–719
Printed in Great Britain

The perturbed region behind a diffracting shock wave

By B. W. SKEWS

Department of Mechanical Engineering, University of the Witwatersrand

(Received 9 January 1967)

The results of an experimental study of the diffraction of shock waves on plane-walled convex corners are given for a Mach number range from 1·0 to 5·0. The behaviour of the disturbances produced in the region perturbed by the corner are discussed. It is shown that the position of the slipstream and tail of the Prandtl–Meyer fan, and the velocities of the contact surface and second shock become independent of corner angle for angles greater than 75°. Comparisons with theoretical predictions of Jones, Martin & Thornhill (1951) and Parks (1952) are included. In most cases fair agreement is obtained.

1. Introduction

In a previous paper (Skews 1967) comparisons were made of the shape of a shock wave diffracting on convex corners, with the predictions of Whitham's (1957) theory. This theory ignores the effect of the perturbed region behind the shock. The region is bounded by the curved part of the incident shock, the wall, and a reflected sound wave (see figure 1). A number of disturbances generally

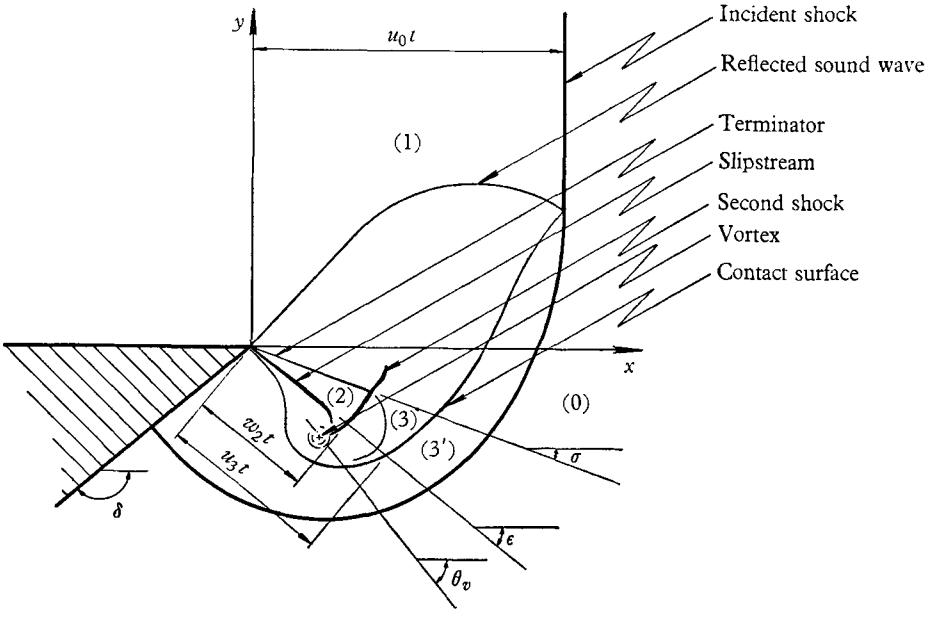

FIGURE 1. Features of the diffraction pattern.

occur within this region and are identified in this figure. The study of the behaviour of these disturbances is the subject of this paper.

A number of tests were conducted during each of which five photographs of the flow pattern were taken at different times. It was established that, within the experimental accuracy and over the range of times and Mach numbers tested, the phenomenon is similar to itself in time; i.e. it is pseudo-stationary. The discussion following can thus be confined to the effect of Mach number and wall angle without considering the history of the process.

Except for the smaller corner angles (15, 30 and 45°) the overall pattern remains qualitatively the same for any given shock Mach number. It is therefore convenient to discuss, first, the effect of Mach number and then the effect of wall angle, where this alters the pattern.

2. The effect of Mach number

A number of schlieren photographs are given in figures 2, 3 and 4 (plates 1, 2 and 3). (The wavy lines visible over the whole field of view in some of these photographs are interference fringes and should be ignored.)

For very weak incident shocks the phenomenon is uncomplicated (figure 2*a*). The reflected sound wave generated at the corner propagates upstream into the slowly moving gas caused by the incident shock and the shock curvature starts where this reflected wave interacts with it. The region perturbed by the corner appears fairly uniform and no steep density gradients are visible. Since the shock is very weak the process is essentially isentropic and the contact surface is not visible. A relatively small vortex is detectable at the corner. The radius of curvature of the diffracted shock is nearly $a_0 t$ and the phenomenon approaches that of a diffracting sound wave.

The features of the flow are not altered significantly as the Mach number increases to 1·2 (figure 2*b*). The reflected sound wave does not propagate upstream as rapidly as in the previous case because of the greater velocity of the oncoming gas. The point of intersection between the reflected wave and the incident shock has, as expected from Whitham's theory, increased in angular elevation as seen from the corner. The contact surface is barely visible and its position cannot be established with any degree of certainty. The vortex is more marked and has propagated slightly further from the corner owing to the higher gas velocity. An interesting feature at this stage of the process is the appearance of the slipstream—this is just visible between the corner and the vortex. The slipstream is the visible evidence of the inability of the shock-accelerated gas to negotiate the corner.

A further stage in the development of the process is shown in figure 2*c*, where $M_0 = 1{\cdot}5$. The contact surface is fairly well defined and its lower end is wound around the vortex. The slipstream is clearer than before and its extremity is also bent towards the vortex as is to be expected. On the upper surface of the slipstream a number of wavelets are apparent. They are roughly perpendicular to the slipstream direction and are the initial stages in the formation of the second shock. At a slightly higher Mach number (see, for example, the colour photo-

graph, figure 4*b*, where $M_0 = 1{\cdot}6$) the second shock has formed and it should be noted that it has not propagated as far from the corner as the vortex. A further increase in M_0 (see the following two colour pictures, $M_0 = 1{\cdot}87$) results in a situation where the second shock and the vortex interact in a rather complex fashion. In these photographs a second radial discontinuity issuing from the corner and situated above the slipstream is visible. This line has been called the terminator. At this Mach number the second shock is bounded by the slipstream and terminator.

At $M_0 = 2{\cdot}0$ (figure 2*d*) the reflected wave can hardly propagate upstream at all since the gas velocity behind the incident shock is nearly sonic. The contact surface, second shock and slipstream are well defined, it again being noted how they are affected by the vortex circulation. The vortex centre is no longer as clearly defined as it was previously.

When $M_0 > 2{\cdot}068$ the gas behind the incident shock becomes supersonic and the reflected sound wave can no longer propagate upstream, but is swept downstream, and the effect of the corner can only be felt within the Mach angle. Figure 2*e* clearly shows this effect for a nominal shock Mach number of 3·0. Other differences in feature noticeable in this figure are that the terminator is very marked and extends all the way from the corner to the second shock, which it no longer limits in length. The terminator is interpreted as being the tail of the Prandtl–Meyer fan (see §5). The vortex appears rather diffuse and the position of its centre can no longer be determined. A band starting from the intersection of the terminator and the second shock and curving around the vortex is noticeable.

At higher Mach numbers no new features appear although the positions of the various discontinuities shift slightly (see, for example, figure 2*f* for $M_0 = 4{\cdot}0$).

3. The effect of wall angle

The diffraction pattern described above is modified at small corner angles. Figure 3*a* (plate 2) shows the shock diffraction on a 15° corner at the same nominal Mach number as figure 2*b*. It is apparent on comparing these results that the only changes in the pattern are that the vortex is much less marked and no slipstream is visible. Similar comparisons at $M_0 = 1{\cdot}5$ show the following two main differences. First, there is no sign of the second shock being formed, and, secondly, the contact surface terminates at the wall. At $M_0 = 2{\cdot}0$ the second shock has formed and the terminator is clearly defined.

In figure 3*b* ($M_0 = 3$) all the general features noted in figure 2*e* are present except for the vortex and slipstream. The boundary layer does not separate from the wall in this case. The terminator is clearly visible although its position is very much different from that occurring at large corner angles. The second shock and contact surface are, to all intents and purposes, in contact with the wall, the contact surface being curved near the wall. At $M_0 = 2{\cdot}0$, $\delta = 30°$ (figure 3*c*) the second shock has a lambda configuration and the start of the boundary-layer separation is distinguishable. Some indication of the presence of the vortex is also

visible. In figure 3*d* separation occurs at the corner and the contact surface is more highly curved than for the previous case. It is as if this discontinuity had been rolled up against the wall and under the vortex.

Figure 3*e* shows the diffraction with $M_0 = 4$ and a corner angle of 45°. Here the folding under of the contact surface against the wall can clearly be seen. Furthermore, the terminator and slipstream originate at a point on the wall slightly downstream of the corner. It thus appears that the boundary layer remains attached to the wall for a short distance before separating and the expansion at the corner is no longer centred.

Figure 3*f* shows the result for $M_0 = 3{\cdot}0$ and a 60° corner. It is seen that the wall is clear of the disturbances and the pattern is similar to that for the larger corner angles.

The general behaviour of the diffraction pattern having been established, detailed analyses and comparisons with the theoretical predictions will now be given.

4. The slipstream

From the experimental records it is clear that the slipstream is due to the separation of the gas and is brought about by the inability of the flow to negotiate the corner. The slipstream is not a sharp discontinuity in the flow but rather a narrow region in which the high-velocity gas on the upper side interacts with the almost stationary gas below it. The width of the region increases as it propagates further from the corner and is generally wider and more turbulent in nature at the smaller corner angles (compare figures 2*d* and 3*d*).

The slipstream is essentially straight and radial over most of its length and only becomes curved at the part furthest from the corner where it is influenced by the presence of the vortex.

The angle at which the slipstream occurs will depend on the pressure to which the flow expands, which, in turn, is dependent on the corner angle.

In order to compare the results for the various corners all are given together in figure 5. 'Best fit' curves are drawn through the results for the 30, 45, 60 and 75° corner angles. For the larger corners a single experimental curve is drawn since the slipstream angle appears to reach a limit and becomes independent of corner angle.

For the 30° corner, $M_0 > 2{\cdot}0$, the slipstream position is nearly independent of shock Mach number, being about 3° from the wall. It was for this angle that it was sometimes noted that the slipstream did not originate at the corner. When the second shock is forming, a lambda configuration appears (see figure 3*c*), the one branch meeting the wall at a point slightly below the corner. The boundary layer remains attached to the wall up to this point and then separates. The point of separation appears to the oncoming flow as a concave corner and an oblique shock results. This shock then merges with the second shock, thereby forming the configuration noted. Where this delayed separation occurs at higher Mach numbers the oblique shock does not appear. This situation is also sometimes apparent at the higher Mach numbers for the 45° corner. An excellent example is given in figure 3*e*—both the slipstream and terminator originate at

a point slightly downstream of the corner. The slipstream and terminator remain straight and the expansion fan can no longer be centred.

For the 45° corner the slipstream angle takes a value between 32° and 35° for $M_0 > 3{\cdot}0$. Over this range the curve is not as insensitive to Mach number changes as is the case for the 30° corner. Increasing the corner angle to 60° gives a slipstream angle much closer to the limiting curve but following the same trend as exhibited by the previous corner.

At 75° a slight change in the shape of the curve becomes apparent, namely that a slight hump in the curve is exhibited in the region of $M_0 = 1{\cdot}5$. Between Mach numbers of 2·5 and 4·0 the slipstream angle may, within the experimental accuracy, be grouped with the remaining corners. After $M_0 = 4{\cdot}0$ this curve also apparently peels away from the limiting case.

The slipstream angles for the 90° to 165° corners appear to be independent of corner angle, within the scatterband of the plotted results. The hump exhibited near $M_0 = 1{\cdot}5$ is very much more pronounced than previously and it is unlikely that this is due to inaccurate measurements of the records. It should be noted, however, that at the lower Mach numbers the slipstream is relatively short and thus prone to larger errors than is the case at higher speeds.

A particularly interesting feature exhibited by the slipstream angle results is the tendency for a limiting condition to be reached. As the second shock is well clear of the wall for corners greater than 60° the situation at the wall approaches that predicted by Jones *et al.* (1951) and it is reasonable to compare the situation they proposed with the experimental behaviour of the slipstream. Their model corresponds to expanding the flow, through a Prandtl–Meyer wave, from the pressure behind the incident shock back to that in front of the shock; i.e. the pressure along the slipstream is p_0 and there is a region of uniform flow above and parallel to it. The interferogram of Griffith & Brickl (1953) shows that, near the wall, the pressure at the slipstream is indeed p_0, although it is lower further away. This dropping off in pressure is due to the presence of the vortex and cannot be allowed for in the theory. The low-pressure area caused by the vortex action is also the reason for the slipstream becoming curved in this region. The theoretical curve is given in figure 5. The agreement is very good over the whole range of Mach numbers for which the theory applies, i.e. $M_0 > 2{\cdot}068$. There appears to be a tendency for the slipstream angle to be lower than that predicted theoretically for $M_0 > 4{\cdot}0$. Tests would have to be conducted at considerably higher Mach numbers in order to confirm this trend.

It should be noted that Griffith & Brickl did not find the limiting condition given above for the three corners they tested, although for the larger corners their results do tend to group at slightly larger angles than predicted theoretically. The discussion of the behaviour of the terminator (§5) gives further reason to believe that this limit is real.

The theoretical limit is obtained by assuming the whole region between the slipstream and the wall to be at pressure p_0 and the diffracted portion of the shock to be sonic. It has been established that this is not the case (Skews 1967). The shock strength is still finite and the pressure immediately behind it is greater than p_0. However, the pressure drops to p_0 at the slipstream owing to the two-dimensional

nature of the flow. The agreement of the theoretical model with experiment is thus confined to the region near the slipstream and not to that near the shock wave.

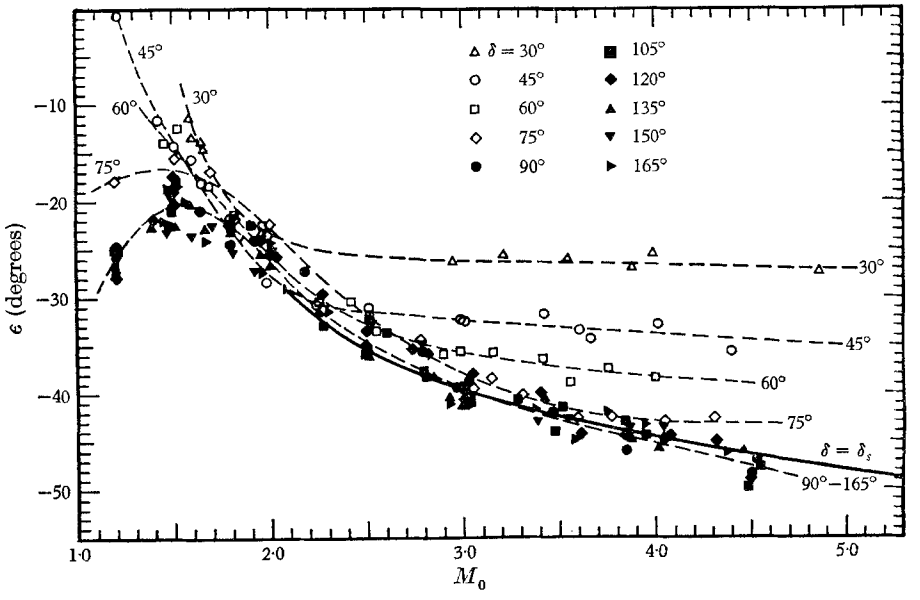

FIGURE 5. Slipstream angle variation with shock Mach number.

The theory does not predict separation at the smaller corner angles where such separation does, in fact, occur. This discrepancy is probably due to the second shock and vortex being in close proximity to the wall, thereby altering the pressure conditions for separation and resulting in the potential flow solution being inapplicable. As the incident shock Mach number decreases so the quasi-steady flow behind the shock becomes slower. For very slow speeds it would be expected that a subsonic potential flow solution is approached and the gas should be able to negotiate a larger angle before separation. This consideration may contribute to the hump noted in the curve at low Mach numbers.

5. The terminator

From the discussion given above it is apparent that the model of Jones *et al.* (1951) applies to the diffraction process in the region of the slipstream. It is therefore to be expected that there is a limited region of uniform flow between the slipstream and the last characteristic of the Prandtl–Meyer fan (the terminator).

The terminator angle was found, in all cases, to be a monotonically decreasing function with increasing shock Mach number. The results for all the corners are plotted together in figure 6. It is noted that the terminator angle approaches some limiting condition with increasing corner angle, as was found for the slipstream angle. At the lower Mach numbers this limiting condition is reached even at the smaller corner angles, the curves for those corners then branching away from the main curve at high Mach numbers.

The theoretical terminator angle may be simply calculated from Prandtl–Meyer theory. The results of such calculations for corner angles of 15° and 30° are shown in figure 6. The calculation assumes that the flow after the corner is at the corner angle. As expected the agreement for the 15° corner is excellent,

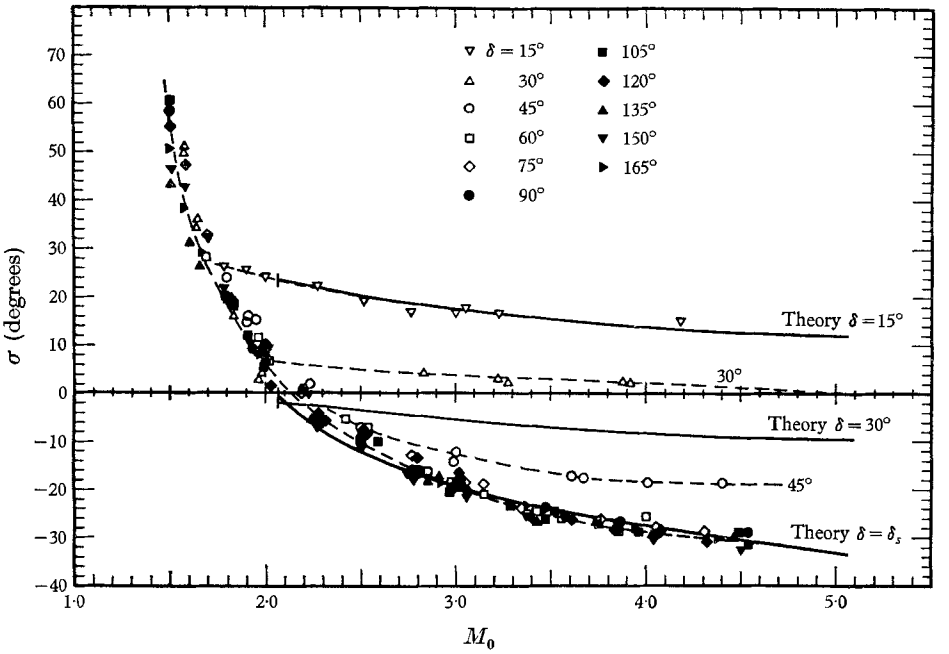

FIGURE 6. Terminator angle variation with shock Mach number.

whereas that for the 30° corner is poor. This is simply because the flow remains attached to the wall for the smaller corner and the corner angle is identical with the flow direction, whereas for the 30° corner a slipstream is visible and the flow, separated from the wall, is at an angle different from the corner angle. Calculation using the experimentally obtained slipstream angles instead of the corner angle should result in much better agreement.

This argument is shown to be sound by the comparisons of the limiting curve in figure 6. Here the theoretically predicted slipstream angle (δ_s), which gave fair agreement with the experimental values, was used in determining the terminator angle. The resulting curve shows excellent agreement with the experimental results for corner angles greater than 60°. This agreement implies that the slipstream does, in fact, exhibit the limit discussed in the previous section. The larger scatter there is probably due to inaccuracies in measurement resulting from the width of the slipstream.

From these results, therefore, there seems to be no doubt that there is a region of uniform flow between the slipstream and the terminator, as was suggested by Jones *et al.* This region is terminated closer to the corner than suggested by these authors because of the presence of the second shock; however, between

this shock and the corner their model gives excellent results. The weakness of Jones's theory is the inability to predict the slipstream and thus the terminator angles at the smaller corners (e.g. 30°).

One further item that requires clarification regarding the behaviour of the terminator is the continuation of the experimentally determined curves to well below $M_0 = 2{\cdot}068$, i.e. into the region where the quasi-steady flow behind the incident shock is subsonic. The existence of the terminator in this region may be explained as follows. The reflected sound wave which propagates upsteam of the corner when $M_0 < 2{\cdot}068$ is an expansion process and thus will accelerate the gas towards the corner.

Extrapolating the experimental curve for the terminator to give a 90° angle (i.e. sonic conditions) gives an incident shock Mach number in the region of 1·45. This corresponds to a Mach number behind the shock of $M_1 = 0{\cdot}56$. In order to achieve sonic conditions by expanding the flow isentropically from this value requires the pressure at the corner to be expanded to $0{\cdot}65p_1$. It appears quite feasible for the reflected expansion wave to achieve this pressure ratio. Unfortunately no means are at present available to the author to confirm that this expansion does in fact occur. Lighthill's (1949) linearized theory shows that low pressures are to be expected at the corner if the angle is small. This has been confirmed by experiment (Fletcher, Weimer & Bleakney 1950).

6. The second shock

The calculations given by Parks (1952) for the two-shock situation on a 30° corner have been extended to other corner angles. From the photographic records it is clear that the two-shock theory is only strictly applicable to the 15° corner, where the second shock remains in contact with the wall. The results for this corner together with the theoretical prediction are presented in figure 7*a*. It is noted that the agreement is good at the lower Mach numbers but as the Mach number increases so the two curves diverge; the actual velocity being higher than that predicted theoretically.

For the 30° angle the discrepancy between the two curves is more marked (figure 7*b*). The experimental results obtained by Parks are included in this figure and show good agreement with the present results. As separation of the boundary is beginning at this corner angle it was expected that the theory would be less accurate.

The experimental results for all the corners are given together in figure 7*c*. This graph is a lot more densely populated than it appears because of the plotted points obscuring each other. These results tend to give a single limiting curve particularly at low Mach numbers. For higher Mach numbers and corners less than 75° the curves diverge from the limiting curve. This result is not surprising considering the behaviour of the slipstream and terminator. As far as the second shock is concerned the effective wall angle is the slipstream angle and the process remains the same. Using this argument as a basis the theoretical velocity of the second shock was calculated using the two-shock theory and the theoretical corner angles for separation (δ_s). This result is compared with the experimental

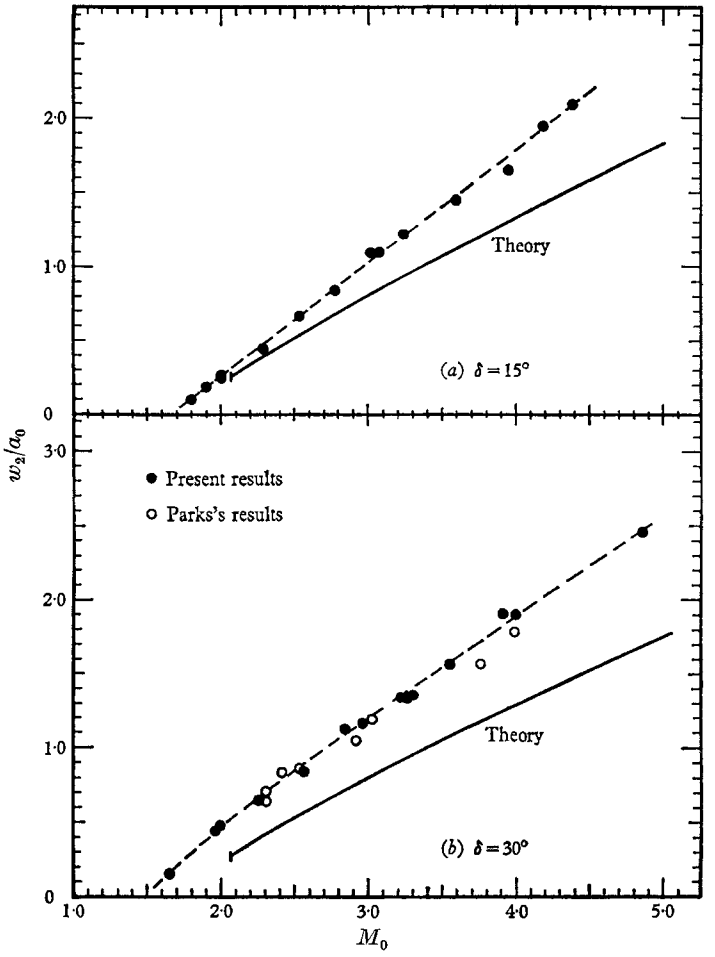

FIGURES 7*a* and 7*b*. Second shock velocity variation with shock Mach number.

values in figure 7*c*. The two-shock theory is inadequate in fully explaining the behaviour of the second shock. The discrepancy is probably due to the coarseness of the assumptions on which the two-shock theory is based; in particular the assumption that the flow along the wall (or slipstream) may be treated as being one-dimensional. It has been established that the region bounded by the slipstream, terminator and second shock is a uniform flow region parallel to the slipstream, and since the second shock is approximately perpendicular to the slipstream the assumption of one-dimensionality is warranted in this region.

It is in the region between the second shock and the incident shock (regions 3 and 3′, figure 1) that the assumption appears to be at fault. In the first place the slipstream is not present in this region, having terminated at the vortex, and there is no reason to believe that the flow is still essentially radial. As the second shock faces upstream the pressure on the downstream side is higher. At the slipstream the pressure is p_0 and the higher pressure behind the shock would result in a two-dimensional flow from this high-pressure region. The proximity of the low-pressure vortex region would aggravate this tendency. Secondly,

neither the contact surface nor the incident shock is perpendicular to the slip-stream direction. Finally, the photographic records clearly show curved density gradients just downstream of the incident shock (see, for example, figures 3*e* and *f*). These disturbances appear to form part of the vortex pattern and give a definite indication of the two-dimensional nature of the flow in this region.

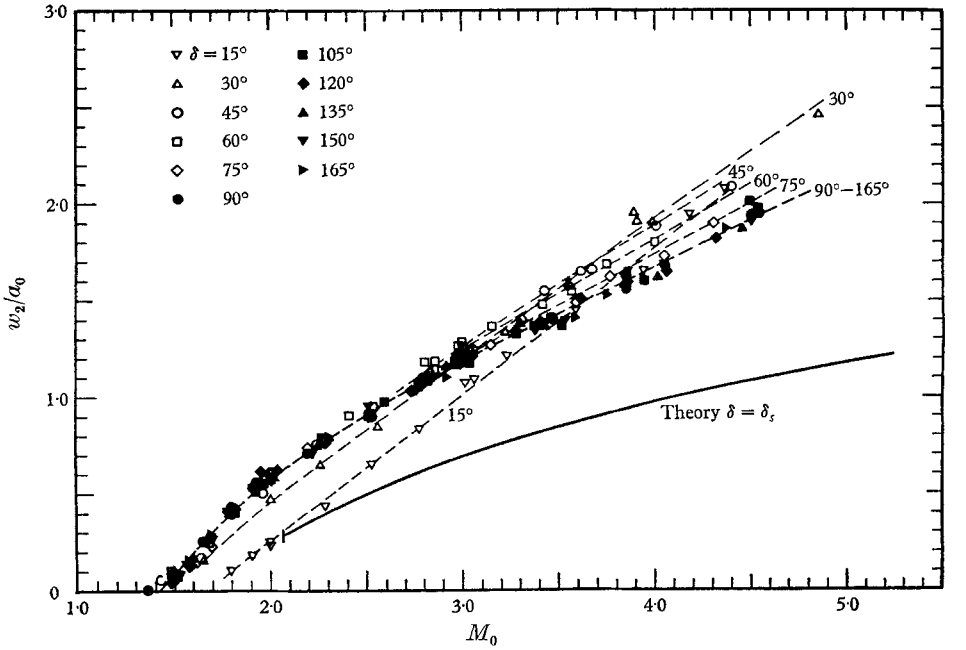

FIGURE 7*c*. Second shock velocity variation with shock Mach number.

It should be noted here that, in the next section where contact surface velocities are considered, much better agreement is obtained with the two-shock theory. The inadequacy of this theory is mainly confined to the second shock behaviour.

In discussing the behaviour of the terminator it was argued that for the terminator to exist below $M_0 = 2{\cdot}068$ it requires that the reflected expansion wave accelerates the flow to sonic conditions on the lower wall, at some point near the corner. The same argument may be applied to the formation of the second shock. For the second shock to exist the Mach number ahead of, and relative to it, must be greater than sonic. Thus when the second shock reaches vanishing strength the velocity of the gas into which it faces must be just sonic. From figure 7*c* it is seen that the second shock velocity becomes zero at a Mach number of about 1·45. This value agrees with that obtained from the terminator behaviour.

This conclusion does not apply to the 15° corner. Here the second shock becomes vanishingly weak in the region $1{\cdot}6 < M_0 < 1{\cdot}7$ (figure 7*a*) and no conclusions could be drawn from the terminator results for this corner. It thus appears that the process is somewhat different owing to the flow not being expanded to a sufficiently low pressure to cause separation.

It is interesting to note the manner in which the second shock forms and how its shape varies for the different corners. For the large corners, tests conducted at low second shock velocities ($M_0 \simeq 1{\cdot}5$) generally show a number of small wave-

lets. These wavelets are mostly perpendicular to the slipstream and are relatively short. The situation appears to be identical with that occurring when sonic speed is exceeded on a solid boundary in plane flow. In the present case too, a small increase in the shock Mach number causes the wavelets to form a single shock. For any given Mach number this shock then grows in a pseudo-stationary manner.

At the lower Mach numbers where the terminator angle is positive the second shock is visible as far as the terminator. At its lower end it is bounded by the vortex. At Mach numbers where the terminator becomes negative the upper end of the second shock remains approximately along the x-axis. At the higher Mach numbers the terminator extends from the corner up to the second shock and is generally well defined over its whole length. At the point where these waves meet, the second shock is more sharply defined and its shape is affected by the interaction; a very slight bulge, facing towards the corner, being noted.

A further point of interest is the manner in which the second shock and vortex interact—this is very clearly shown in the colour photographs (figures 4*c* and *d*, plate 3) for $M_0 = 1{\cdot}9$. Before this interaction the vortex is more sharply defined, but thereafter it becomes more and more diffuse as the Mach number increases (compare figures 4*a* and 4*b* with 4*e* and 4*f*). This interaction should preferably be studied with the aid of an interferometer so that the pressure distribution of the vortex can be obtained.

At the smaller corner angles (15° and 30°) the descriptions given above no longer apply. For the 30° corner the original formation of the second shock from wavelets occurs in the same manner as for the larger corners, although at a slightly higher Mach number. The boundary layer separates at the corner and a broad region of turbulence is noted. At a slightly higher Mach number the wavelets combine to give a well-defined second shock. This shock is considerably larger than that occurring on larger corners at the same Mach number. It is noted that the flow separates beyond the corner. At the point of separation a compression wave, which becomes an oblique shock, is formed. At slightly higher Mach numbers this situation persists, although the second shock becomes very much shorter. Further increases in Mach number cause the oblique shock to become weaker and eventually to die away. From this stage onwards increases in Mach number result in trends similar to those exhibited at larger angles.

The results for the 15° corner are again different. This may be expected, as the boundary layer does not separate, no slipstream is formed, and the second shock is either in contact with the wall or in very close proximity to it. In none of the tests were the wavelets apparent. The first indication of the appearance of the second shock is in the region $M_0 = 1{\cdot}6$, although its presence is difficult to assess because of the proximity of the vortex. Increasing the shock Mach number results in the second shock increasing in length and velocity. No peculiarities in behaviour were noted at any stage. In all cases the upper end of the shock stops in the vicinity of the terminator.

7. The contact surface

The contact surface originates at the point of intersection of the reflected sound wave and the incident shock (figure 3*c*). However, in the vicinity of this point it is very weak and diffuse as entropy gradients in the flow are small. As

one moves down the contact surface away from this point the entropy gradients increase. The lower entropy changes for the weaker shocks also explain why the contact surface is not clear for tests at low Mach numbers (figures 2*a* and 2*b*).

For the 15° corner the contact surface is in contact with the wall at all Mach numbers. The two-shock theory may thus be expected to give reasonable predictions of its velocity. The comparison is given in figure 8*a*. The agreement is good. It is noted that the contact surface is not perpendicular to the wall as

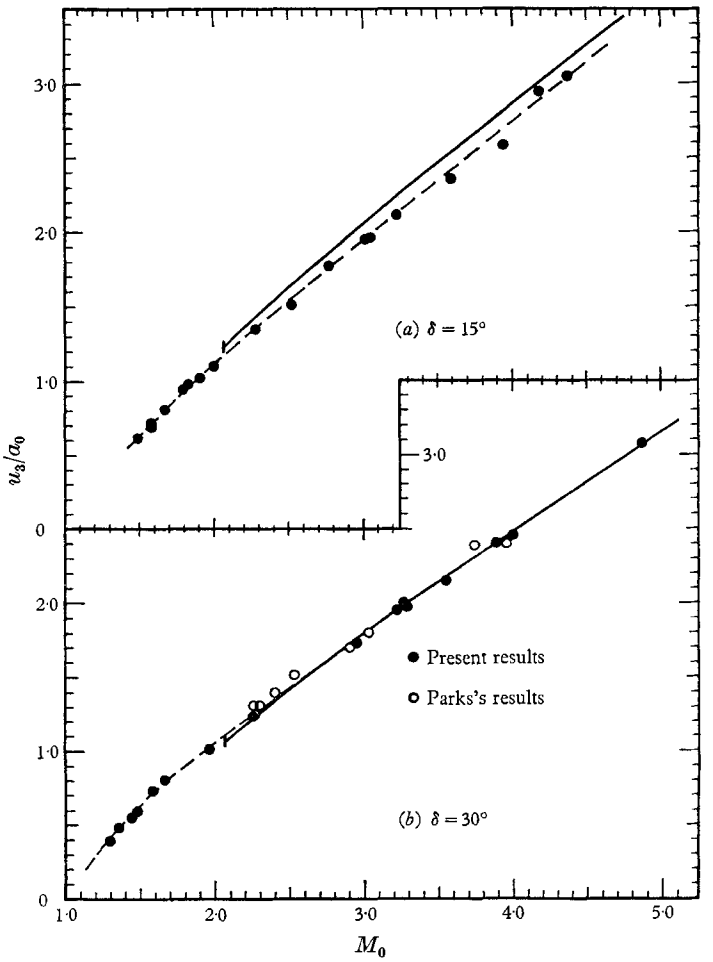

FIGURES 8*a* and 8*b*. Contact surface velocity variation with shock Mach number.

is required by the theory. Furthermore, as the Mach number increases so the contact surface becomes more and more curved in the vicinity of the wall. This, first, results in difficulty in determining precisely where the contact surface strikes the wall, and, secondly, causes increasing deviation from the theoretical model.

The curvature of the contact surface at the wall is more marked for the 30° corner, although it still terminates at the wall (figure 3). The situation here is complicated because of the separation of the boundary layer and the appearance of the slipstream. Velocities determined at the wall will be significantly lower than

those determined along the slipstream direction because of the high curvature. The velocities along the slipstream direction and the theoretical prediction for this corner are given in figure 8*b*. It is surprising that the agreement is as good as it is. This agreement may be largely fortuitous, considering that obtained for the second shock behaviour. Parks's results are also shown on this figure and give good agreement.

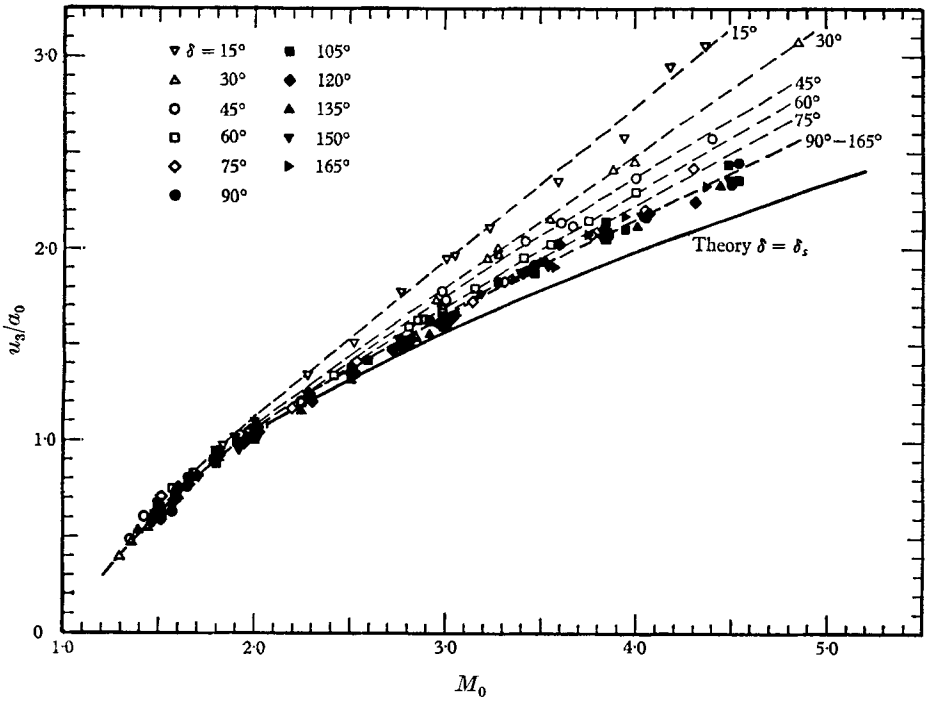

FIGURE 8*c*. Contact surface velocity variation with shock Mach number.

The contact surface is highly curved for the 45° corner; in fact at the higher Mach number this curvature results in the surface not terminating at the wall but rather lying along it, as if it were rolled out owing to the action of the vortex. The velocities that are determined are therefore those along the slipstream direction. At the larger corner angles the effect of the vortex system is even more noticeable, the presence of the wall apparently having little effect on the phenomenon (see figure 2*d*, for example).

At the large angles the contact surface appears to be swept around the vortex, but, as it approaches the slipstream, it suffers a sudden change of direction and then is essentially straight until it reaches the corner. Since the contact surface moves at particle velocity this shape gives a good idea of the gas movement. The process between the wall shock and the corner is thus originally one of compression (across the shock) followed by one of expansion, such that the gas immediately below the corner, between the slipstream and the wall, is stationary. This coincides with the conclusion of §4 and is borne out by the interferogram given by Griffith & Brickl (1953).

As the slipstream acts as the effective wall, as far as the two-shock theory is concerned, the theoretical contact surface velocities were calculated along this

line. The result is presented in figure 8*c*, together with the experimental results. As is to be expected the experimental velocities appear to be independent of corner angle for corners greater than 90°. The agreement between the theoretical velocities and these limiting velocities is fair and the comments given in the previous sections regarding the validity of the two-shock theory along the slipstream direction appear to be confirmed.

The agreement obtained for the contact surface is, however, much better than that obtained for the second shock. This may be partly due to the fact that the second shock velocity is more sensitive to changes in corner angle than the contact surface velocity. Furthermore, the second shock is in close proximity to the vortex, even interacting with it, and will thus be affected by it to a much greater extent than the contact surface.

8. The vortex

If it is assumed that the vortex follows a particle path, then Whitham's theory indicates a curved path. It has been established, however, that the particles comprising the slipstream move along a nearly straight path. As the vortex moves along just below the slipstream it is therefore expected that it should also follow a straight line. This was found to be the case.

The motion of the vortex is described in terms of a vortex velocity q_v and a vortex angle θ_v (measured with respect to the x-axis). The variation of these parameters with shock Mach number are shown in figure 9. The scatter in the results is due to the difficulty in pinpointing the centre of the vortex with any degree of accuracy. The vortex is fairly well defined for $M_0 < 2{\cdot}0$; above this value it spreads out over a fairly broad region and involves the contact surface, the slipstream and the lower end of the second shock.

At the lower end of the Mach number range ($M_0 < 1{\cdot}5$) the vortex velocity is always higher than the second shock velocity. For corners greater than 105° the vortex velocity is equal to the second shock velocity at about $M_0 = 1{\cdot}75$, and at higher Mach numbers is slightly lower. For corners between 90° and 45° the vortex velocity becomes the same as the second shock velocity near $M_0 = 2{\cdot}0$ and, from the four results obtained at higher Mach numbers, apparently remains at the second shock velocity over the remainder of the range. No definite conclusion can be reached for the 30° angle because of the scatter in the results. No measurable vortex is apparent for the 15° corner.

It was noted that the angle between the vortex and slipstream directions becomes smaller as the Mach number increases. Although this trend is apparent for all the corners where a vortex is present it is mainly noticeable at the lower Mach numbers.

The vortex angle appears to approach a limit for corner angles greater than 105°. In these cases the angle increases rapidly at low Mach numbers and becomes less sensitive to Mach numbers at the higher values. The same trend is exhibited for the 105° corner and, to a lesser extent, for the 90° case. For the remaining walls the dependency is weak and, because of the scatter, is not determinable. All that can be said for these cases is that the vortex angle increases with corner angle.

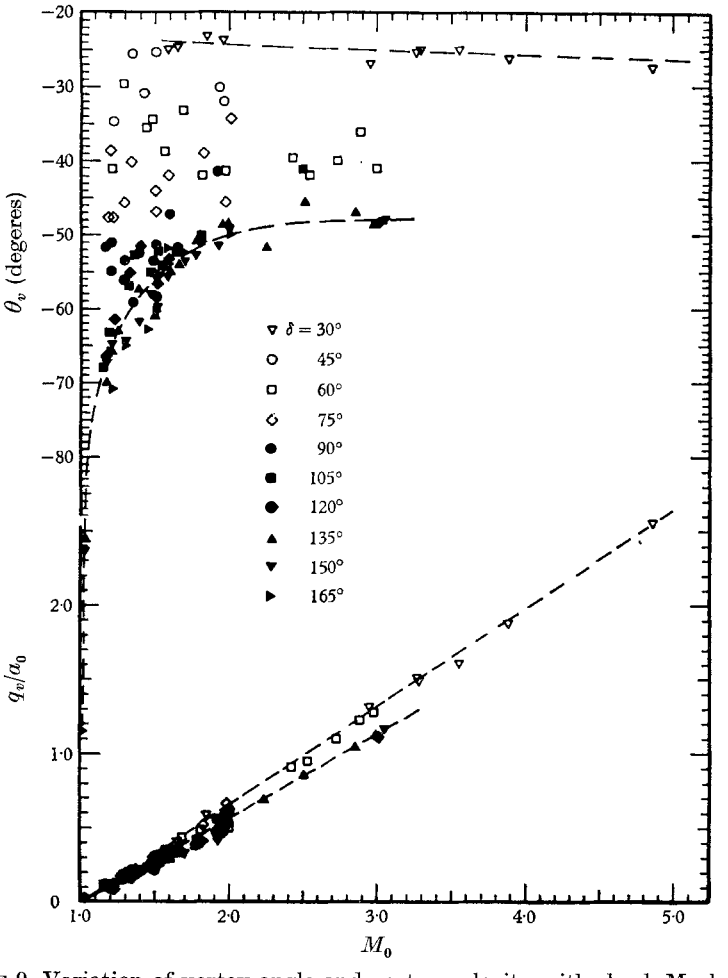

FIGURE 9. Variation of vortex angle and vortex velocity with shock Mach number.

The superimposed results for the vortex velocity show a much more consistent grouping. The dependency appears to be nearly linear for all corners, with the slope on the curve slightly greater for the smaller corner angles. The vortex velocity is thus only weakly dependent on corner angle. There is an indication of a limiting condition being reached for corner angles greater than 90°.

An interferometric study would appear to be necessary in order to obtain more reliable information on the vortex behaviour.

REFERENCES

FLETCHER, C. H., WEIMER, D. K. & BLEAKNEY, W. 1950 *Phys. Rev.* **78**, 634.

GRIFFITH, W. & BRICKL, D. E. 1953 *Phys. Rev.* **89**, 451.

JONES, D. M., MARTIN, P. M. E. & THORNHILL, C. K. 1951 *Proc. Roy. Soc.* A **209**, 238.

LIGHTHILL, M. J. 1949 *Proc. Roy. Soc.* A **198**, 454.

PARKS, E. K. 1952 *University of Toronto, Institute of Aerophysics, UTIA Rept.* no. 18.

SKEWS, B. W. 1967 *J. Fluid Mech.* **29**, 297.

WHITHAM, G. B. 1957 *J. Fluid Mech.* **2**, 145.

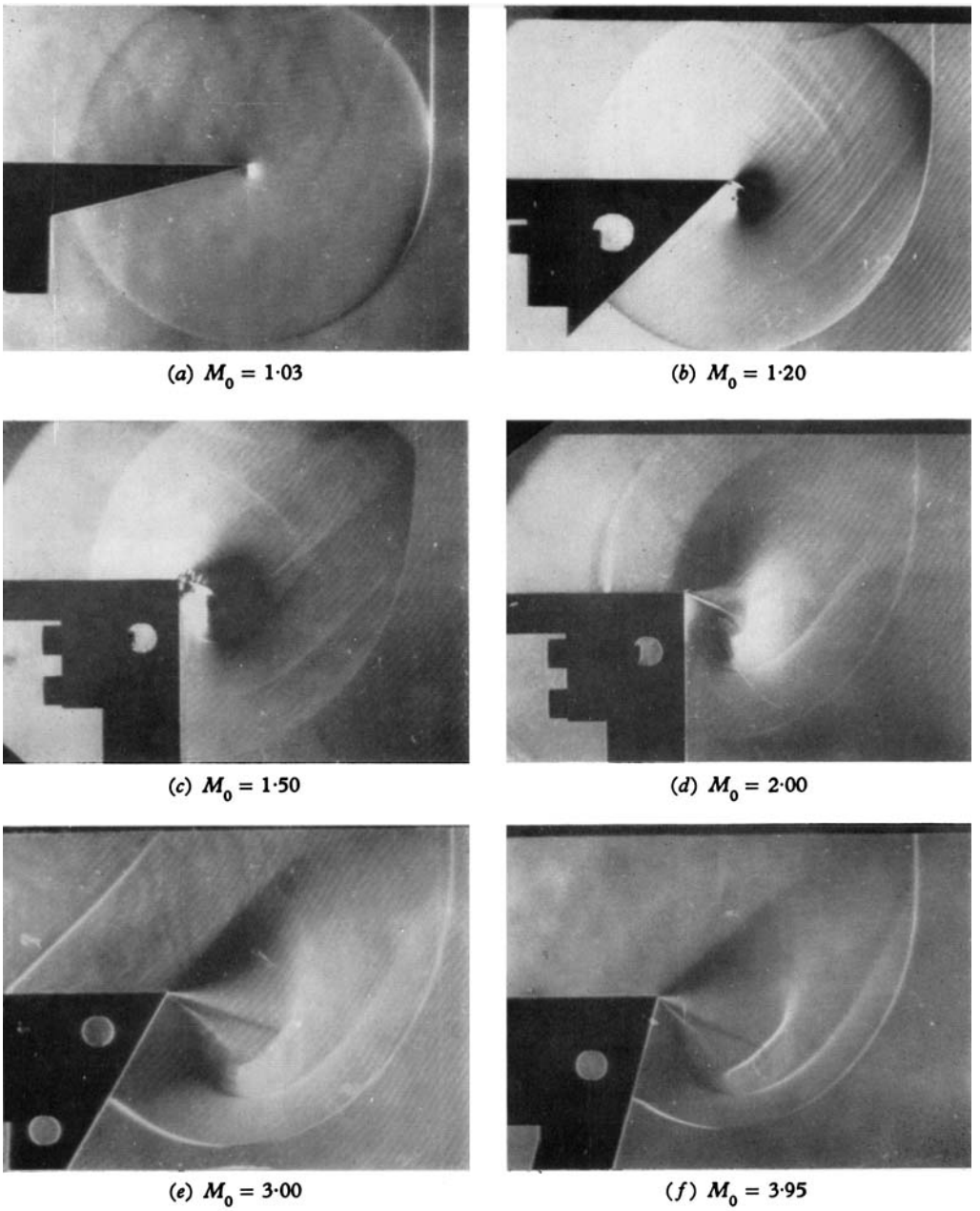

FIGURE 2. Schlieren photographs (large corner angles).

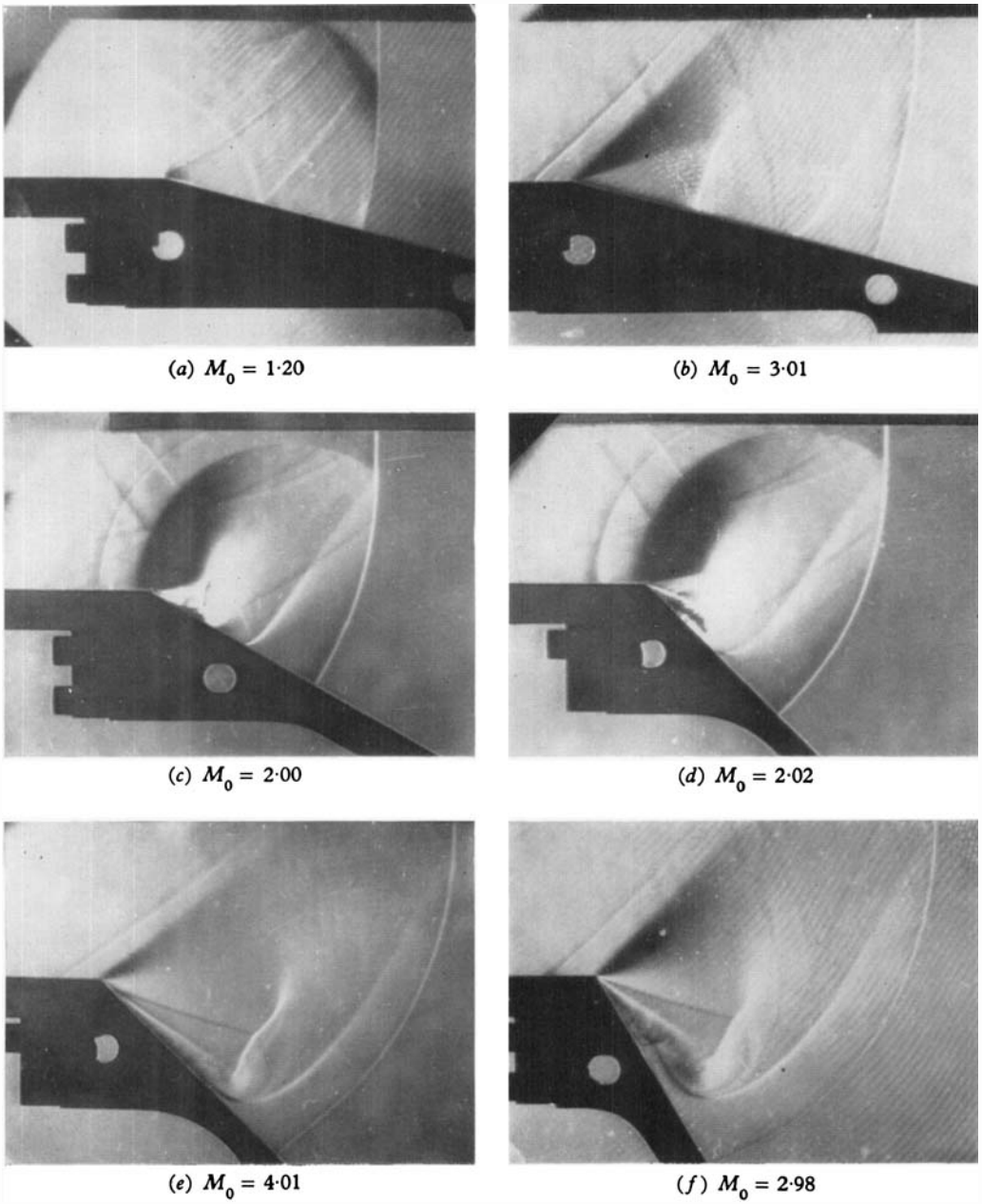

FIGURE 3. Schlieren photographs (small corner angles).

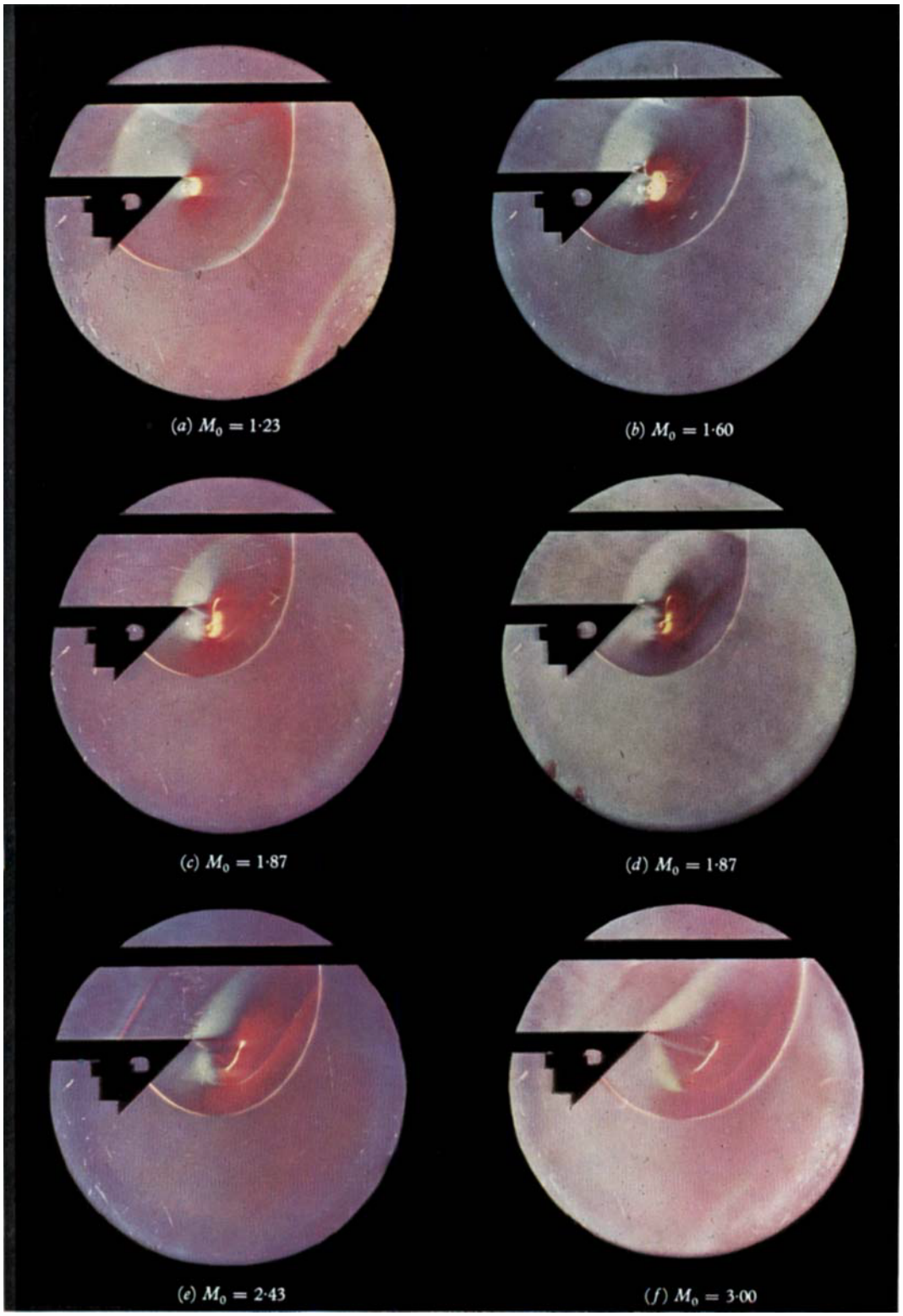

FIGURE 4. Colour schlieren photographs. (*a*) $M_0 = 1.23$, (*b*) $M_0 = 1{\cdot}60$, (*c*) $M_0 = 1{\cdot}87$, (*d*) $M_0 = 1{\cdot}87$, (*e*) $M_0 = 2.43$, (*f*) $M_0 = 3{\cdot}00$.